Check for updates

Titanium carbide ceramic nanocrystals to enhance the physicochemical properties of natural rubber composites

J. M. A. R. B. Jayasinghe, [ID] [abc] Rangika T. De Silva,[b] K. M. Nalin de Silva, [ID] [a] Rohini M. de Silva [ID] *[a] and Vinod Asantha Silva[c]

The mechanical strength of natural rubber (NR) was enhanced by incorporating novel titanium carbide (TiC) nanocrystals as a filling material. The rubber nanocomposites were prepared through mixing TiC nanoparticles with NR latex and the resulting NR/TiC masterbatch was further mixed at the solid stage with other chemicals *via* internal mixing. The final rubber composites prepared using TiC as the nanofiller were denoted as NR/TiC-0, NR/TiC-0.5, NR/TiC-1.0, NR/TiC-2.5, and NR/TiC-5.0; moreover, a comparative study was conducted using carbon black (CB-330) as the filler and the composites were denoted as NR/CB-1.0 and NR/CB-5.0. As per the results of tensile tests, the NR/TiC-1.0 composite revealed the highest tensile value of 31.13 MPa and this indicated improvement by 92% compared to that of the control (NR/TiC-0 (16.22 MPa)); moreover, it indicated improvements by 73% and 63% compared to the values of NR/CB-1.0 and NR/CB-5.0, respectively. Moreover, scanning electron microscopy (SEM) analysis revealed a better dispersion of the NR/TiC-1.0 composite compared to the other composites. Furthermore, dynamic mechanical analysis (DMA) was conducted to observe the energy storage and loss properties at dynamic conditions; the results revealed that the highest storage peak and lowest loss peak were observed for the NR/TiC-1.0 composite. Also, thermogravimetric analysis revealed the superior thermal stability of the NR/TiC-1.0 composite to that of the others at the NR degradation temperature of around 400 °C. Importantly, the curing time (t_{90}) of NR/TiC-1.0 was reduced considerably compared to that of the other composites even the NR/CB composites, which would be beneficial for industries to save energy at the curing stages of tire-like applications. The improvements were significant when compared to the industrially well-known NR/CB composites and well above the industrially required minimum parameters of the tire industry. Ultimately, this will open up a distinct avenue for natural rubber reinforcement.

Introduction

Reinforced natural rubber-based composites are being widely used in a vast number of applications such as tires, conveyor belts, and thermal pads.[1–11] The desired properties of rubber for these applications are being achieved by incorporating typical reinforcing fillers such as carbon black (CB) and silica. Nevertheless, in recent times, the research community has been focusing on new types of filler materials to prepare superior rubber composites to CB and silica-based composites. Among these, ceramic materials are an effective solution to challenge the superior properties of CB or silica-based rubber composites due to their definite properties than conventional fillers.

Ceramic materials are well known in the composite technology field because of their use in applications such as transducers,[12] semiconductors,[13] batteries,[14] sensors, and mechatronic devices.[15] Among the ceramic materials, titanium carbide (TiC) is a well-known ceramic reinforcing agent in metal composites due to its high wear resistance, melting point, and elastic modulus and relatively low coefficient of thermal expansion.[16–19] TiC-based metal composites have been prepared by blending with nickel and iron alloys for high-temperature applications due to their high thermal stability (melting point: 3065 °C).[20] Moreover, Dong *et al.* prepared nickel and steel metal composites with high wear resistance by incorporating very low volume fractions (0.35 and 0.45, respectively) of TiC particles.[21] This shows the possibility of obtaining the desired material properties even with a small loading of TiC. Other than metal composites, several polymers blended with TiC have also been reported. Chairman *et al.* prepared TiC-based glass-epoxy composites to prevent the two-body abrasive wear behavior observed during sliding applications, and a considerable

[a] *Centre for Advanced Materials and Devices (CAMD), Department of Chemistry, University of Colombo, Colombo 00300, Sri Lanka. E-mail: rohini@chem.cmb.ac.lk*

[b] *Sri Lanka Institute of Nanotechnology (SLINTEC), Nanotechnology and Science Park, Pitipana, Homagama 10206, Sri Lanka*

[c] *Global Rubber Industries, Perawala Estate, Badalgama 11538, Sri Lanka*

improvement was obtained even at 2.0 wt% loading.[22] The use of synergistically reinforced TiC and nitrogen-doped graphene with epoxy composites to prepare high-performance microwave absorbers has revealed that the TiC-based composites are highly promising fillers for dielectric and electromagnetic applications.[23] Apart from the epoxy-based composites, elastomeric reinforcement using certain ceramic fillers such as boron nitride (BN) and silicon carbide[24,25] (SiC) has been commonly used in the last decade. Additionally, Farid El-Tantawy studied the thermal conductive properties of a TiC/ethylene-propylene-diene monomer (EPDM) composite using micron range (8 μm) TiC particles and improved thermal conductivity was obtained at a significantly high loading of the TiC filler (0–20 phr); however, significant attention has not been given to the physical properties of the composite.[26] It is worth noting that no one has considered the preparation of rubber composites using nano-scale TiC particles and the study of their physical properties with the reinforcement behavior.

Solid tires are used in the material handling industry, where the tires are exposed to heavy loads. Structurally, solid tires are composed of three main layers, *i.e.*, tread, center, and base; the initiation of failure mainly arises at the center and base layers due to the generation of considerable heat and low mechanical properties. Therefore, it is very important to reduce the heat generation as well as strengthen the mechanical properties in order to stop the frequent failure of solid tires. In this research, we have prepared NR/TiC (NR – natural rubber) masterbatches through latex mixing, followed by melt mixing to disperse other chemicals and curatives. The main objective of this work is to enhance the physical properties of the natural rubber composites by incorporating a minor amount of a nanoscale filler to prepare commercially viable, less heat generating and high strength rubber compounds. This research would be beneficial to solid rubber tire manufacturers to fabricate tires with enduring centre and base layers.

Experimental section

Materials and methods

Nano titanium carbide (TiC) (size – 40 nm, purity ≥95.0%) was purchased from Luoyang Tongrun Info Technology Co. Ltd., China. Triton X-100 (purity ≥99.0%) was used as a surfactant to prepare the TiC dispersion, and it was purchased from Glorchem Enterprise Pvt. Ltd, Sri Lanka. For comparison purposes, carbon black grade (CB) N-330 was purchased from Phillips Carbon Black Limited India. Centrifuged natural rubber latex (NRL) with 60% dry rubber content (DRC) was purchased from Hanwella Rubber Products Pvt. Ltd, Sri Lanka. Other chemicals for the preparation of the vulcanized rubber composite such as zinc oxide (ZnO) (99.5%), stearic acid (SA), *N-tert*-butyl-benzothiazole sulfonamide (TBBS), tetramethyl thiuram monosulfide (TMTM), and insoluble sulphur were industrial grade chemicals and all chemicals were used as received without further purification.

Preparation of the TiC water dispersion

This nanopowder was dispersed in a deionized water medium with the aid of the surfactant to ease the mixing with NRL. As per the optimized conditions, 0.5% (w/w) TiC dispersion was prepared as follows. Initially, 0.5 g of Triton X-100 was dissolved in 99.5 mL of deionized water and it was stirred for 20 min to obtain a water surfactant homogenous mixture. Then, 0.5 g of TiC nanopowder was added and mixing was continued for another 20 min to disperse TiC in the water medium using a mechanical mixer (400 rpm). Then, it was ultrasonically deflocculated to break up any agglomerates using a Hielscher UP50H – Compact Lab Homogenizer at 60% amplitude for 10 min. After this, other dispersions such as 1.0%, 2.5%, and 5.0% (w/w) TiC dispersions were prepared using the same procedure.

Preparation of TiC/NR masterbatch *via* latex mixing

First, 166.7 g (dry rubber content (DRC)-60%) of NRL was added to an initially prepared TiC water dispersion to obtain NR/TiC-0.5, NR/TiC-1.0, NR/TiC-2.5, and NR/TiC-5.0 composites. For instance, 100.0 ml of 0.5% (w/w) TiC dispersion was added to 166.7 g of NRL and stirred for 20 min to obtain a homogeneous mixture, which was further ultrasonically flocculated for 2 min to make sure that all flocculated TiC agglomerates were broken. Afterward, the suspension was poured into medium size (176 mm × 250 mm) aluminum plates and quickly coagulated using 2.5% (w/v) formic acid to avoid any settlement of the dispersed particles. The coagulated sheets were passed through a two-roll mill to squeeze out excess water. After that, the nip gap of the two-roll mill was reduced to obtain 2 mm-thick rubber sheets to ease the oven drying process. The prepared sheets were kept in the oven at 65 °C for 72 h to obtain a dried NR/TiC masterbatch and finally stored in a desiccator.

Preparation of vulcanized NR/TiC rubber composites

The NR/TiC composite was prepared through melt mixing using an internal mixture (HAAKE Polylan OS RheoDrive 7, Thermo SCIENTIFIC) and the resulting rubber chunk was sheeted using a two roll milling system. The mixing chamber was preheated to 80 °C and the Banbury rotter speed was set to 60 RPM. Thereafter, the NR/TiC masterbatch, chemicals, and curatives were added within 0, 1.5 and 3 min time intervals and subsequently, the mixture was dumped after 6 min of total mixing time. The curing time of each composite was measured using an oscillating disk rheometer (EKTRON EKT2000 Rotorless Rheometer) at 150 °C and the cured sheets (2 × 100 × 100 mm) were prepared using a hydraulic heating press at 150 °C as per the curing time of each composite. The total solid rubber content of each mixture was 100 phr and the detailed formulations are given in Table 1.

Characterization

Physical properties

Tensile properties. A tensile testing machine (Instron Model 3365) was utilized to evaluate the ultimate tensile stress and modulus of each sample at a 500 mm min^{-1} test speed according to ASTM D412. The thickness of each sample was

Table 1 Compounding formulations of NR/TiC composites

Formulation	NR/TiC-0	NR/TiC-0.5	NR/TiC-1.0	NR/TiC-2.5	NR/TiC-5.0	NR/CB-1.0	NR/CB-5.0
Gum rubber	100.00	—	—	—	—	—	—
TiC master batch	—	100.50	101.00	102.50	105.00	—	—
CB master bach	—	—	—	—	—	101.00	105.00
Zinc oxide 99.5%	4.00	4.00	4.00	4.00	4.00	4.00	4.00
Stearic acid	2.50	2.50	2.50	2.50	2.50	2.50	2.50
TBBS	1.00	1.00	1.00	1.00	1.00	1.00	1.00
TMTM	0.30	0.30	0.30	0.30	0.30	0.30	0.30
Sulphur	1.50	1.50	1.50	1.50	1.50	1.50	1.50
Total	**109.30**	**109.80**	**110.30**	**111.80**	**114.30**	**110.30**	**110.30**

measured using a digital micrometer screw-gauge (Mitutoyo, 0.001 mm resolution).

Rebound resilience

The rebound resilience of each sample was conducted as a percentage value according to ASTM D2632 – 01 using a rubber rebound resilience elasticity tester (Hefei Fanyuan Instrument Co. Ltd).

Hardness test

The hardness value of each composite was measured using a durometer (bareiss, BS 06) (shore A) according to ASTM D2240 – 15. The average value of 10 different points was reported to achieve more accurate results.

Crystalline nature

X-ray diffraction (XRD) (Rigaku SmartLab SE, Japan) was utilized to analyze the crystalline nature of the neat TiC sample and TiC/NR nanocomposite. The pattern was recorded with Cu Kα radiation (40 kV, 100 mA, $\lambda = 0.154$ nm) between 5° and 90° with a step size of 0.04°. All samples were tested at room temperature without any further activation.

Morphological analysis

The surface morphology of neat TiC and NR/TiC-1.0 composites was carried out by field-emission scanning electron microscopy (SEM) (Hitachi SU6600). Each sample was coated with gold to prevent electrostatic charging during the observation.

Rheological properties

The rheological behavior of the prepared rubber composites was obtained using an oscillating disk rheometer (EKTRON EKT2000 Rotorless Rheometer) as per ASTM D2084/D5289. The testing temperature and the oscillating arc angles were set at 150 °C and 0.5°, respectively, prior to implementing the test. Subsequently, the minimum torque (S_1), maximum torque (S_2), scorch time t_2, and optimum curing time (t_{90}) were evaluated using the rheograph (torque *vs.* time) of each composite.

Dynamic mechanical analysis

Dynamic mechanical tests were performed by using a Perkin Elmar DMA 8000 instrument operating in dual cantilever mode at a frequency of 1 Hz and an amplitude of 50 μm from −70 to 80 °C. The sample was 7 mm in width, 2.0 mm in thickness, and 10 mm in length. The heating rate was 3 °C min^{-1}. The storage modulus (E'), loss modulus (E''), and loss factor (tan δ) were evaluated.

Results and discussion

Cure characteristics

The curing behavior of the prepared rubber nanocomposites was analyzed at 150 °C using MDR and the obtained scorch time (t_2), cure time (t_{90}), maximum torque (S_1), and minimum torque (S_2) values are summarized in Table 2. The curing time of the neat TiC composite (NR/TiC-0) was 12.36 min and was the highest curing time among all the composites. This can be attributed to the absence of the filler TiC in the matrix. The lowest t_{90} value obtained for NR/TiC-1.0 (7.88 min) revealed the better heat distribution in the NR matrix around the TiC particles, showing the presence of a large amount of filler polymer interactions.[9]

Usually, the filler in the matrix enhances the thermal conductivity of the composite and leads to efficient heat transfer into the polymer matrix to cure the sample. This mechanism was clearly evident in our experiment, where the curing times of the composites loaded with TiC were reduced significantly compared to that of the neat NR sample. Even though we expected decreased curing times on increasing the TiC loading, our results revealed the lowest curing time for the NR/TiC-1.0 composite. This could be ascribed to the optimal ratio between TiC and NR to obtain the

Table 2 Curing properties of TiC/NR composite

Formulation	S_1 (lbf in)	S_2 (lbf in)	ΔS (lbf in)	t_2 (min)	t_{90} (min)
NR/TiC-0	1.95	13.39	11.44	6.98	12.36
NR/TiC-0.5	2.56	13.86	11.30	4.85	8.96
NR/TiC-1.0	1.78	13.07	11.29	4.39	7.88
NR/TiC-2.5	1.79	13.43	11.64	5.15	9.12
NR/TiC-5.0	1.42	13.12	11.70	5.49	9.68

best dispersion of the TiC nanoparticles throughout the matrix when compared to the other higher loaded composites. This observation was in very good agreement with the SEM and tensile measurements. The SEM image of NR/TiC-1.0 shows very uniform distribution of the TiC particles and this can be credited to the enhanced thermal conductivity, as previously reported.[27] In the NR/TiC-5.0 composite, the level of the agglomeration of TiC was very high and the distribution was very irregular with significant microscopic agglomeration. Moreover, the scorch time (t_2) indicated the same trend as t_{90} and there was better scorch safety for all the prepared composites. Delta torque ($\Delta S = S_2 - S_1$) was measured considering the difference in the maximum torque (S_2) and minimum torque (S_1) obtained from MDR and this value was in good agreement with the predicted cross-linking density of the prepared composites.[28] For instance, NR/TiC-1.0 had the lowest ΔS value (11.29 lbf in) compared to the other composites, indicating that it had the highest cross-linking density. In general, lower ΔS reflects lower cross-linking density and lower tensile strength. However, the NR/TiC-1.0 composite had the highest tensile strength and the lowest ΔS value compared to other composites. This indicates that the tensile strength might not utterly depend on the cross-linking density and may also arise from better polymer filler interactions.

Mechanical properties

The ultimate tensile strength (UTS), tensile modulus at 10% elongation (M10), and elongation at break (EB) of the NR/TiC nanocomposites are illustrated in Fig. 1. As per Fig. 1a, all the composites exhibit the typical stress–strain behavior of visco-elastic materials, as reported previously.[29–31] The slope of each curve increased with strain, and the slope sharpened after 600% elongation. This could be due to the typical strain-induced crystallization of natural rubber.[32] The UTS values of each composite are shown in Fig. 1b, where the tensile strength increased up to 1 phr of TiC loading and eventually, the trend was reversed. The UTS values of NR/TiC-0.5, NR/TiC-1.0, NR/TiC-2.5, and NR/TiC-5.0 improved by 57%, 92%, 76%, and 22%, respectively, compared to that of the control. Most importantly, NR/TiC-1.0 showed a significant improvement in its UTS value compared to all other composites. Moreover, this tensile pattern was clearly observed even at low strains (<10%), as shown in inset 1.0 in Fig. 1a. Significantly, all the stress–strain curves were smooth and we could not observe any irregularity at any loading, reflecting the absence of macroscopic level agglomerates in the matrix. The presence of humps in the curve indicates the existence of macroscopic-level filler–filler
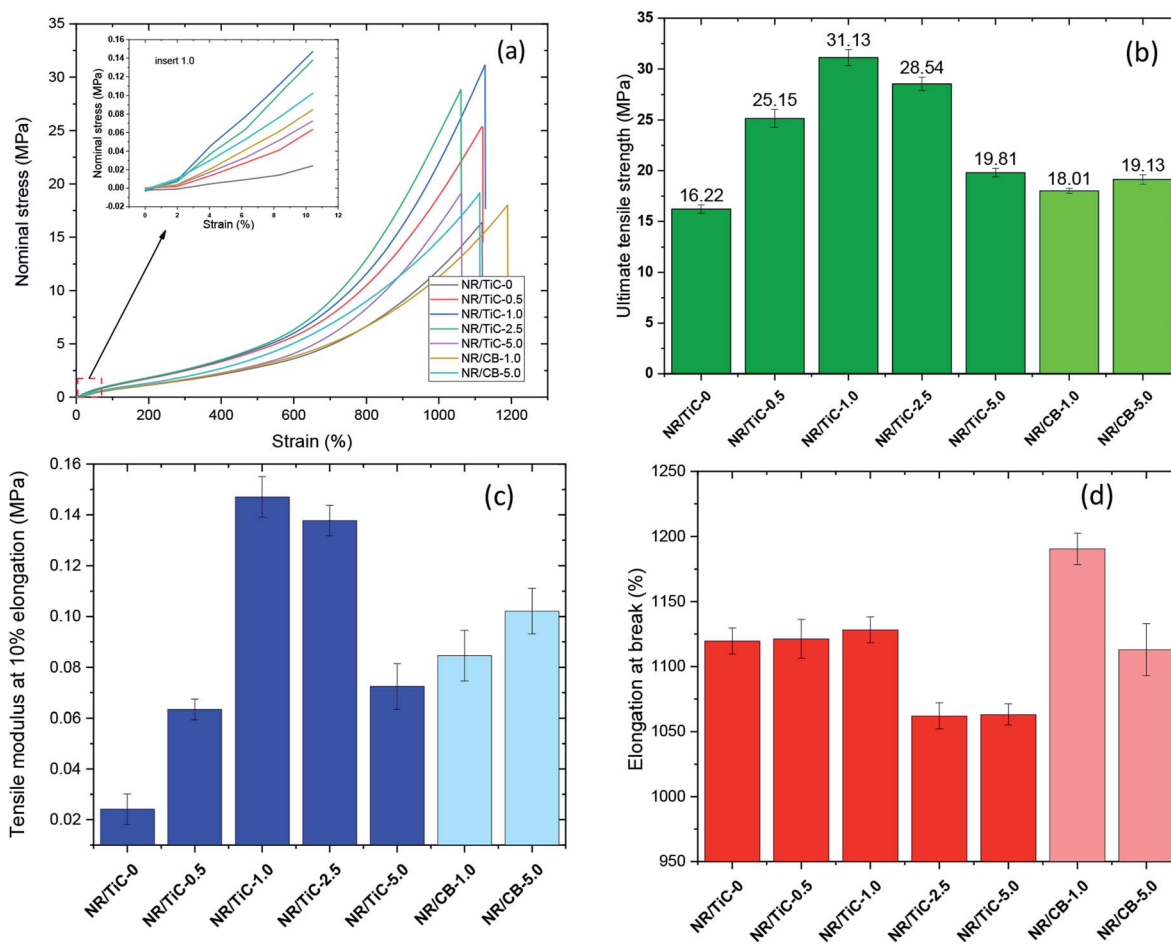

Fig. 1 (a) Nominal stress vs. strain (%) (b) maximum tensile strength of the composites (c) tensile modulus at 10% elongation and (d) elongation at break of the prepared composites.

interactions (van der Waals interactions between agglomerates) in the matrix. For comparison, two other samples were prepared using conventional CB-330 grade with 1 phr and 5 phr loadings (denoted as NR/CB-1.0 and NR/CB-5.0, respectively), and their UTS values were 18.01 and 19.1 MPa, respectively. These values were comparable only to that of the NR/TiC-0 composite. On the other hand, the UTS of the NR/TiC-1.0 composite improved by 73% and 63% compared to NR/CB-1.0 and NR/CB-5.0, respectively. Generally, the tensile strength of a filled rubber composite is mainly attributed to the interactions between the filler and polymer interfaces. Normally, strong filler polymer interactions at the interface will restrict the mobility of the polymer chains on the filler surfaces. However, with higher filler loadings, the filler–filler interactions rather than the filler matrix interactions will be higher, and this tends to result in large filler aggregates throughout the matrix at the microscopic level. At higher stress conditions, the stress of the matrix or main polymer will transfer to the filler particles through the filler polymer interface. Therefore, the presence of less filler–polymer interactions at higher filler loadings can facilitate the breakpoints of the composite at lower stress values.[33] Therefore, a uniform distribution of the filler inside the rubber matrix is very important to reduce stress-focused areas and deliver better mechanical properties.[34] In this regard, it can be assumed that the dispersion of TiC is homogenous up to 1 phr loading, and further increase in the TiC loading tends to result in microscopic aggregates similar to those seen in the SEM micrograph of NR/TiC-5.0 (Fig. 4c). Fig. 1c illustrates the tensile modulus at 10% elongation, where NR/TiC-1.0 exhibits a higher value compared to the NR/TiC and NR/CB composites. Even at low elongations, the higher modulus values confirm the better filler matrix compatibility throughout the entire range of linear deformation. The elongation at break (EB) values of the rubber composites are shown in Fig. 1d. As per the results, the EB of TiC/NR-1.0 (1121%) was almost the same as that of the control (1120%) and further increase in the loading of TiC up to 2.5 phr and 5.0 phr led to reduction in EB to 1062% and 1063%, respectively. As previously reported, the EB of rubber composites mainly depends on the elastically active polymer segments

of the matrix.[35] TiC/NR-0 consisted of the most elastically active polymer segments due to the absence of any filler components. Remarkably, the TiC/NR-1.0 composite showed similar EB to that of the control and this may be due to the better reinforcement of the matrix rather than blocking the active elastic portion of the matrix. Therefore, the TiC/NR-1.0 composite revealed simultaneous enhancement in both UTS and EB. The significant increase in the elongation at break of the NR/CB composites compared to that for the NR/TiC composites can be attributed to the inferior interfacial interactions of this surfactant-mediated dispersion method. However, the tensile strengths of the NR/CB composites were significantly lower and therefore, this cannot be considered as an instance of greater reinforcement. The rebound resilience of the prepared rubber nanocomposites is depicted in Fig. 2a and the trend did not significantly change up to 1.0 phr loading of TiC. However, there was a considerable reduction in resilience at higher loadings. The rebound resilience of the composites is inversely proportional to the loss properties (energy loss) of the composites.[36] Therefore, the results revealed that the energy loss of the NR/TiC composites at small loadings was not significant and the hysteretic loss became more noteworthy at higher TiC loadings. These results were further confirmed through DMA. Due to the aggregation of filler particles at higher filler loadings, the applied energy is lost at the filler interface due to weak van der Waals forces and this part of the composite is well identified as viscous.[37]

The determination of shore hardness is a fast and accurate method to determine the hardness of rubber composites[38] and the obtained results are depicted in Fig. 2b. As per the results, the hardness of the filler-loaded composites increased slightly compared to that of the control sample and this general behavior can be expected with any non-reinforcing or reinforcing filler component, as reported previously.[39,40]

Dynamic mechanical analysis (DMA)

DMA is used to study the viscoelastic behavior of materials by subjecting the specimen to either constant cyclic stress or strain
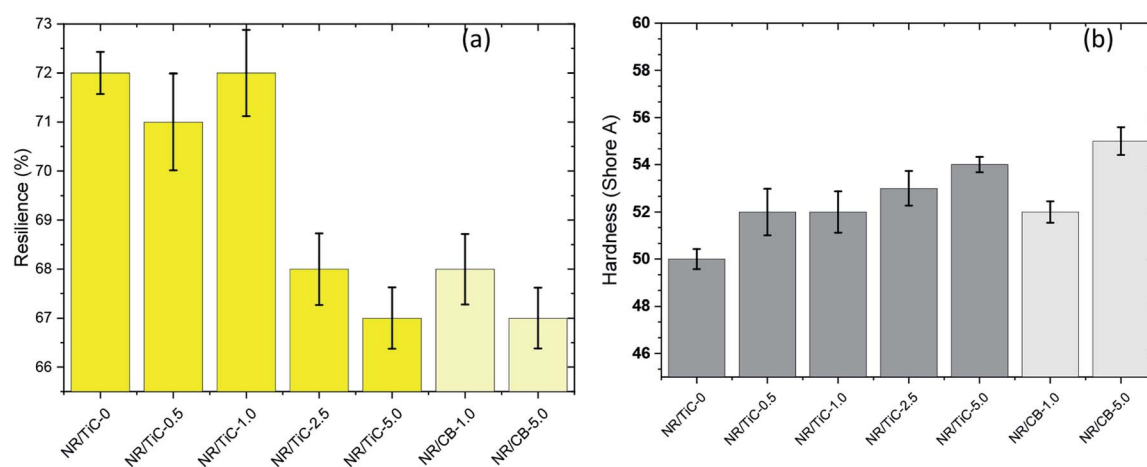

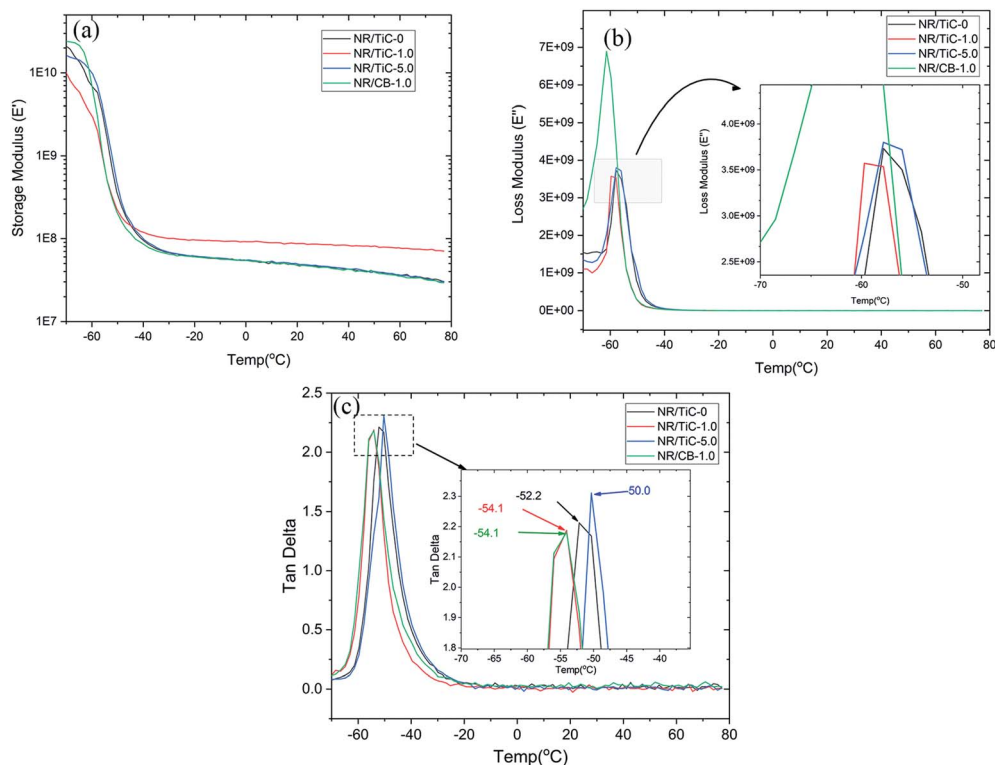Fig. 2 (a) Resilience and (b) hardness of the prepared TiC/NR rubber composites.

Fig. 3 Dynamic mechanical analysis: (a) storage modulus (b) loss modulus (c) and tan delta of the prepared rubber composites.

to measure the resultant stress or strain. In this study, we observed the resultant stress of a sample after subjecting to 50 micron constant strain. As per DMA analysis, the storage modulus (E') (Fig. 3a), loss modulus (E'') (Fig. 3b), and tan δ (Fig. 3c) were recorded over a wide range of temperatures (from −70 °C to 80 °C). The storage modulus (E') or dynamic modulus of the composite indicates the stiffness of the sample and its energy storage capacity for future purposes to expense the energy when required. As shown in Fig. 3a E' for all composites follow a general trend where it shows high E' at low temperatures and low E' at high temperatures. However NR/TiC-1.0 shows a deviation from the other composites having enhanced E' at high temperatures. For comparison, the NR/CB-1.0 composite was analyzed to observe the behavior but it did not coincide with the observation for NR/TiC-1.0. The retaining of a higher elastic portion of the NR/TiC-1.0 composite should be the reason for the enhancement in E'.[37]

Loss modulus (E'') or dynamic loss modulus indicates the damping behavior or energy loss behavior of a particular composite compared to the applied energy. The obtained E'' curves of the composites show a high intense loss peak for the CB/NR-1.0 composite compared to the other composites and this may be due to the filler polymer incompatibility of CB and NR with our latex mixing method, which was used to prepare the TiC/NR nanocomposites. Moreover, among the TiC/NR composites, TiC/NR-1.0 showed the lowest loss peak and this was in agreement with the E' data of this composite. The graph of tan δ of a rubber composite can be directly used to measure the damping behavior as a ratio of loss modulus and storage

modulus (tan $\delta = E''/E'$). This will give an overall idea about the compound behavior over the entire range of temperature. The obtained tan δ graph showed the typical behavior of the rubber compound on increasing the temperature and the highest tan δ peak was obtained at the glass transition temperature (T_g). The T_g values of NR/TiC-0, NR/TiC-1.0, NR/TiC-5.0, and NR/CB-5.0 were −52.2, −54.1, −54.1, and −50.0 °C, respectively. Typically, T_g should increase with particle loading and these results revealed that T_g decreased on increasing the particle loading. As a norm, the flexible part of a polymer is restricted and becomes stiffer with increased filler loading and this should increase the T_g point of the composites. In contrast to this idea, the NR/TiC-1.0 composite showed a lower T_g point than the control sample. However, these results are on par with the insignificant contribution of nanoceramic fillers, which can alter the T_g of the polymer matrix.[41] At the interface, these particles can dramatically alter the chain kinetics of the polymer, which is more closely bound to the filler surfaces. Moreover, the extremely high surface area of the nanofillers even at low loading amounts can provide a large interfacial area, which can alter the bulk properties.[41] Furthermore, extensive studies regarding silica nanoparticle-incorporated composites carried out by Becker and co-workers have revealed reduction in the T_g point with appropriate filler polymer matrix interactions.[42]

SEM analysis

The fracture surface morphology of the prepared composites was determined using SEM and the obtained results are depicted in Fig. 4. Fig. 4a shows the SEM image of the control sample and it
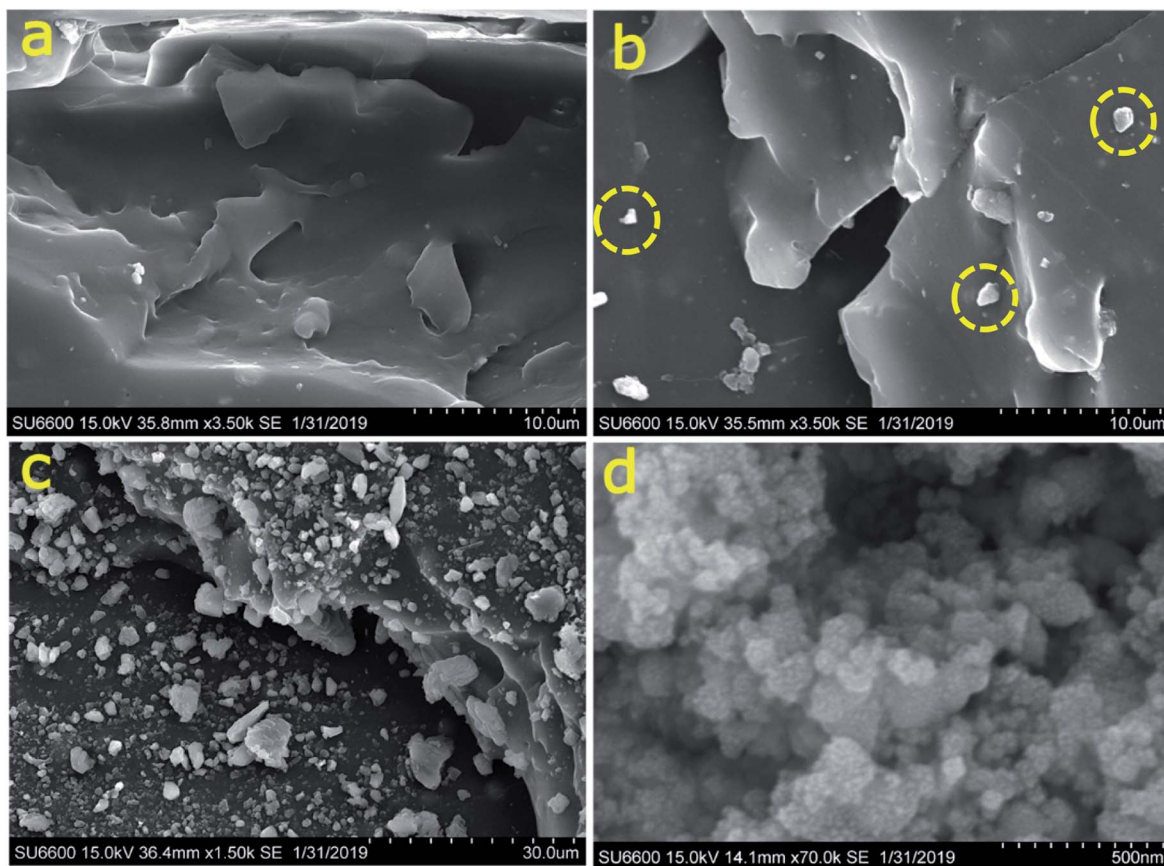
Fig. 4 Scanning electron micrographs (SEM) of the (a) control (NR/TiC-0), (b) NR/TiC-1.0 rubber composite, (c) NR/TiC-5.0 rubber composite and (d) neat TiC nanoparticles.

clearly shows the absence of aggregated particles at the fracture surface. Fig. 4b is similar to that of the control sample but indicates occasional aggregates of TiC (yellow circles). This indicated that TiC was distributed more or less evenly throughout the natural rubber matrix, resulting in better filler dispersion and leading to significant enhancement in the tensile strength of the NR/TiC-1.0 composite compared to the control sample. Similar to our study, the enhancement in mechanical properties owing to the better dispersion of filler materials inside the polymer matrix has been reported previously.[43,44]

The SEM image obtained for a higher loading of TiC, *e.g.*, NR/TiC-5.0 (Fig. 4c) reflects a considerable amount of TiC micro-aggregates, which could have led to poor filler–polymer interactions. As a result, inferior mechanical properties were observed for higher loaded samples compared to that for NR/TiC-1.0.

X-ray diffraction (XRD) analysis

The X-ray diffraction patterns of the neat TiC nanoparticles and prepared rubber nanocomposites are shown in Fig. 5. As shown in the figure, the neat TiC nanoparticles exhibit characteristic 2θ peaks at around $37°$, $42°$, and $62°$, as previously reported.[45,46] Moreover, the XRD pattern of the control sample indicated a characteristic broad peak for natural rubber at around $20°$ and the intensity of this particular peak reduced for the NR/TiC-1.0 composite. Apart from this, few other peaks were observed for
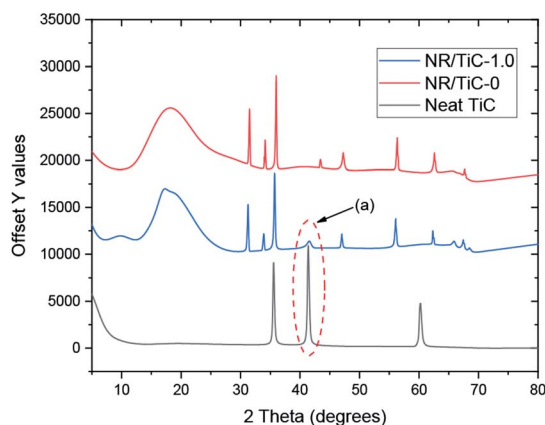

Fig. 5 X-Ray diffractometry study of neat TiC and TiC rubber composites.

both samples, which could be due to other additives that were added during the compounding process. Comparing the control sample with the NR/TiC-1.0 composite, there was a specific peak at $42°$ (Fig. 5, arrow (a)) for NR/TiC-1.0, which corresponded to that for neat TiC, and this showed the presence of TiC nanoparticles in this sample.
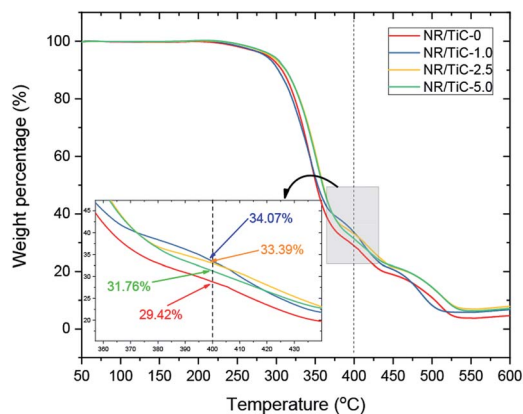
Fig. 6 Thermogravimetric analysis of the TiC rubber nanocomposites.

Thermal properties

The thermal stability of the prepared rubber composites was evaluated using thermogravimetric analysis and the results are depicted in Fig. 6. According to the results, the degradation of natural rubber started at around 300 °C and the control sample degraded rapidly compared to the other TiC-loaded samples. However, increased thermal stability of the NR/TiC composites on increasing the TiC loading was not observed as expected. Instead, the highest thermal stability was exhibited by NR/TiC-1.0, which also showed the best results for other parameters, as mentioned above. This effect was clearly noticeable at around 350–400 °C, where the rapid degradation of natural rubber takes place. For instance, at 400 °C, the remaining weight percentages of NR/TiC-0, NR/TiC-1.0, NR/TiC-2.5, and NR/TiC-5.0 were 29.42%, 34.07%, 33.39%, and 31.76% respectively. Considerably, the percentage improvement for the NR/TiC-1.0 composite compared to NR/TiC-0 was 4.65% and this could evidence the higher reinforcement effect in the natural rubber matrix at 1 phr loading of TiC particles, reflecting the best filler matrix compatibility. After 500 °C, the curves upturned slightly and this could be due to the oxidation of TiC to TiO_2 particles, which has been reported elsewhere.[47]

Conclusion

The physio-mechanical properties of natural rubber, mainly ultimate tensile strength, could be increased using titanium carbide (TiC) as a nanoscale filler. The significant finding was the weight ratio between the matrix and the filler. The ultimate tensile strength of natural rubber improved by 92% even with 1.0 phr particle loading of nano TiC and it improved by 63% compared to the NR/CB-5.0 composite. Moreover, the NR/TiC-1.0 composite showed enhanced properties for other parameters, namely, thermal stability and rebound resilience, which were even better than those of the loaded NR/TiC-1.0 composite. The main reason for these improvements was analyzed using SEM, DMA, TGA, and the rheological data of MDR. The results confirmed that the improvements were due to the best and well-suited particle dispersion through the polymer matrix. This is a new direction to enhance the properties of natural rubber

using ceramic nanomaterials even at small loadings. Therefore, our developed best composite, NR/CB-1.0, revealed excellent mechanical properties and low heat generation compared to the existing rubber composites. Furthermore, the reduced cure time (improved thermal conductivity) can be an additional benefit to save energy, which in turn would help reduce the production cost. Considering all these facts and findings, we can conclude that the developed composite would certainly benefit the solid tire industry to develop low-cost tires with enhanced lifetimes, higher load-bearing capacities, and the ability to operate under harsh environmental conditions.

Conflicts of interest

There are no conflicts to declare.

Acknowledgements

References

1 P. K. Chattopadhyay, S. Chattopadhyay, N. C. Das and P. P. Bandyopadhyay, Impact of Carbon Black Substitution with Nanoclay on Microstructure and Tribological Properties of Ternary Elastomeric Composites, *Mater. Des.*, 2011, **32**(10), 4696–4704.

2 A. Dey, S. Hadavale, M. A. S. Khan, P. More, P. K. Khanna, A. K. Sikder and S. Chattopadhyay, Polymer Based Graphene/Titanium Dioxide Nanocomposite (GTNC): An Emerging and Efficient Thermoelectric Material, *Dalton Trans.*, 2015, **44**(44), 19248–19255.

3 Z. P. Luo and J. H. Koo, Quantification of the Layer Dispersion Degree in Polymer Layered Silicate Nanocomposites by Transmission Electron Microscopy, *Polymer*, 2008, **49**(7), 1841–1852.

4 J. E. Mark, Ceramic-Modified Elastomers, *Curr. Opin. Solid State Mater. Sci.*, 1999, **4**(6), 565–570.

5 S. Salaeh, N. Muensit, P. Bomlai and C. Nakason, Ceramic/Natural Rubber Composites: Influence Types of Rubber and Ceramic Materials on Curing, Mechanical, Morphological, and Dielectric Properties, *J. Mater. Sci.*, 2011, **46**(6), 1723–1731.

6 K. Sankaran, G. B. Nando, P. Ramachandran, S. Nair, U. Govindan, S. Arayambath and S. Chattopadhyay, Influence of Hybrid Nanostructures and Its Tailoring Mechanism on Permeability, Rheology, Conductivity, and Adhesion Properties of a Novel Rubber Blend Nanocomposite, *RSC Adv.*, 2015, **5**(107), 87864–87875.

7 K. Sankaran, P. Manoharan, S. Chattopadhyay, S. Nair, U. Govindan, S. Arayambath and G. B. Nando, Effect of Hybridization of Organoclay with Carbon Black on the Transport, Mechanical, and Adhesion Properties of Nanocomposites Based on Bromobutyl/Epoxidized Natural Rubber Blends, *RSC Adv.*, 2016, **6**(40), 33723–33732.

8 M. J. Wang, S. Wolff and J. B. Donnet, Filler-Elastomer Interactions. Part III. Carbon-Black-Surface Energies and Interactions with Elastomer Analogs, *Rubber Chem. Technol.*, 1991, 714–736.

9 P. K. Chattopadhyay, U. Basuli and S. Chattopadhyay, Studies on Novel Dual Filler Based Epoxidized Natural Rubber Nanocomposite, *Polym. Compos.*, 2010, **31**(5), 835–846.

10 Z. Todorova, N. Dishovsky, R. Dimitrov, F. El-Tantawy, N. Abdel Aal, A. Al-Hajry and M. Bououdina, Natural Rubber Filled SiC and B4C Ceramic Composites as a New NTC Thermistors and Piezoresistive Sensor Materials, *Polym. Compos.*, 2008, **29**(1), 109–118.

11 J. M. A. R. B. Jayasinghe, R. T. De Silva, R. M. De Silva, K. M. N. De Silva, M. M. M. G. P. G. Mantilaka and V. A. Silva, Effect of Networked Hybridized Nanoparticle Reinforcement on the Thermal Conductivity and Mechanical Properties of Natural Rubber Composites, *RSC Adv.*, 2019, **9**(2), 636–644.

12 V. F. Janas and A. Safari, Overview of Fine-Scale Piezoelectric Ceramic/Polymer Composite Processing, *J. Am. Ceram. Soc.*, 1995, **78**(11), 2945–2955.

13 M. Arbatti, X. Shan and Z. Cheng, Ceramic-Polymer Composites with High Dielectric Constant, *Adv. Mater.*, 2007, **19**(10), 1369–1372.

14 Y. Kobayashi, H. Miyashiro, T. Takeuchi, H. Shigemura, N. Balakrishnan, M. Tabuchi, H. Kageyama and T. Iwahori All-Solid-State Lithium Secondary Battery with Ceramic/Polymer Composite Electrolyte, in *Solid State Ionics*, Elsevier, 2002, vol. 152–153, pp. 137–142.

15 K. Li, D. W. Zeng, K. C. Yung, H. L. W. Chan and C. L. Choy, Study on Ceramic/Polymer Composite Fabricated by Laser Cutting, *Mater. Chem. Phys.*, 2002, **75**(1–3), 147–150.

16 Q. C. Jiang, X. L. Li and H. Y. Wang, Fabrication of TiC Particulate Reinforced Magnesium Matrix Composites, *Scr. Mater.*, 2003, **48**(6), 713–717.

17 P. Sahoo and M. J. Koczak, Microstructure-Property Relationships of *in Situ* Reacted TiC/AlCu Metal Matrix Composites, *J. Mater. Sci. Eng. A*, 1991, **131**(1), 69–76.

18 Z. Xiuqing, W. Haowei, L. Lihua, T. Xinying and M. Naiheng, The Mechanical Properties of Magnesium Matrix Composites Reinforced with (TiB$_2$ + TiC) Ceramic Particulates, *Mater. Lett.*, 2005, **59**(17), 2105–2109.

19 K. I. Parashivamurthy, R. K. Kumar, S. Seetharamu and M. N. Chandrasekharaiah, Review on TiC Reinforced Steel Composites, *J. Mater. Sci.*, 2001, **36**(18), 4519–4530.

20 N. Durlu, Titanium Carbide Based Composites for High Temperature Applications, *J. Eur. Ceram. Soc.*, 1999, **19**(13–14), 2415–2419.

21 Ö. Doğan, J. Hawk, J. Tylczak, R. Wilson and R. Govier, Wear of Titanium Carbide Reinforced Metal Matrix Composites, *Wear*, 1999, **225–229**, 758–769.

22 S. P. K. Babu, A. Chairman, N. Mohan and H. Siddaramaiah, Investigation on Two-Body Abrasive Wear Behavior of Tungsten Carbide Filled Glass Fabric - Epoxy Hybrid Composites, *Adv. Mater. Res.*, 2010, **123–125**, 1039–1042.

23 Y. Qing, H. Nan, F. Luo and W. Zhou, Nitrogen-Doped Graphene and Titanium Carbide Nanosheet Synergistically Reinforced Epoxy Composites as High-Performance Microwave Absorbers, *RSC Adv.*, 2017, **7**(44), 27755–27761.

24 K. Kueseng and K. I. Jacob, Natural Rubber Nanocomposites with SiC Nanoparticles and Carbon Nanotubes, *Eur. Polym. J.*, 2006, **42**(1), 220–227.

25 W. Zhou, S. Qi, C. Tu and H. Zhao, Novel Heat-Conductive Composite Silicone Rubber, *J. Appl. Polym. Sci.*, 2007, **104**(4), 2478–2483.

26 F. El-Tantawy, New Double Negative and Positive Temperature Coefficients of Conductive EPDM Rubber TiC Ceramic Composites, *Eur. Polym. J.*, 2002, **38**(3), 567–577.

27 K. H. Solangi, S. N. Kazi, M. R. Luhur, A. Badarudin, A. Amiri, R. Sadri, M. N. M. Zubir, S. Gharehkhani and K. H. Teng, A Comprehensive Review of Thermo-Physical Properties and Convective Heat Transfer to Nanofluids, *Energy*, 2015, **89**, 1065–1086.

28 H. Ismail, S. Tan and B. T. Poh, Curing and Mechanical Properties of Nitrile and Natural Rubber Blends, *J. Elastomers Plast.*, 2001, **33**(4), 251–262.

29 J. M. Chenal, C. Gauthier, L. Chazeau, L. Guy and Y. Bomal, Parameters Governing Strain Induced Crystallization in Filled Natural Rubber, *Polymer*, 2007, **48**(23), 6893–6901.

30 H. Ismail and R. M. Jaffri, Physico-Mechanical Properties of Oil Palm Wood Flour Filled Natural Rubber Composites, *Polym. Test.*, 1999, **18**(5), 381–388.

31 P. M. Visakh, S. Thomas, K. Oksman and A. P. Mathew, Crosslinked Natural Rubber Nanocomposites Reinforced with Cellulose Whiskers Isolated from Bamboo Waste: Processing and Mechanical/Thermal Properties, *Composites, Part A*, 2012, **43**(4), 735–741.

32 S. Toki and B. S. Hsiao, Nature of Strain-Induced Structures in Natural and Synthetic Rubbers under Stretching, *Macromolecules*, 2003, **36**(16), 5915–5917.

33 S. Srivastava and Y. Mishra, Nanocarbon Reinforced Rubber Nanocomposites: Detailed Insights about Mechanical, Dynamical Mechanical Properties, Payne, and Mullin Effects, *Nanomaterials*, 2018, **8**(11), 945.

34 H.-X. Huang and J.-J. Zhang, Effects of Filler-Filler and Polymer-Filler Interactions on Rheological and Mechanical Properties of HDPE-Wood Composites, *J. Appl. Polym. Sci.*, 2009, **111**(6), 2806–2812.

35 F. Grasland, L. Chazeau, J. M. Chenal, J. Caillard and R. Schach, About the Elongation at Break of Unfilled Natural Rubber Elastomers, *Polymer*, 2019, **169**, 195–206.

36 P. S. Oubridge, Physical Properties of Elastomers for Design and Development, *Polym. Test.*, 1987, **7**(5), 325–328.

37 N. Saba, M. Jawaid, O. Y. Alothman and M. T. Paridah, A Review on Dynamic Mechanical Properties of Natural Fibre Reinforced Polymer Composites, *Constr. Build. Mater.*, 2016, **106**, 149–159.

38 M. M. ElFaham, A. M. Alnozahy and A. Ashmawy, Comparative Study of LIBS and Mechanically Evaluated Hardness of Graphite/Rubber Composites, *Mater. Chem. Phys.*, 2018, **207**, 30–35.

39 W. Y. Zhou, S. H. Qi, H. Z. Zhao and N. L. Liu, Thermally Conductive Silicone Rubber Reinforced with Boron Nitride Particle, *Polym. Compos.*, 2007, **28**(1), 23–28.

40 Z. Yang, H. Peng, W. Wang and T. Liu, Crystallization Behavior of Poly(ε-Caprolactone)/Layered Double Hydroxide Nanocomposites, *J. Appl. Polym. Sci.*, 2010, **116**(5), 2658–2667.

41 B. J. Ash, L. S. Schadler and R. W. Siegel, Glass Transition Behavior of Alumina/Polymethylmethacrylate Nanocomposites, *Mater. Lett.*, 2002, **55**(1–2), 83–87.

42 C. Becker, H. Krug and H. Schmidt, Tailoring of Thermomechanical Properties of Thermoplastic Nanocomposites by Surface Modification of Nanoscale Silica Particles, *MRS Online Proc. Libr.*, 1996, **435**(2), 237–242.

43 L. H. Huang, X. Yang and J. Gao, Study on Microstructure Effect of Carbon Black Particles in Filled Rubber Composites, *Int. J. Polym. Sci.*, 2018, **2018**(6), 1–11.

44 N. D. Bansod and C. Das, Studies on Mechanical, Rheological, Thermal and Morphological Properties of *in Situ* Silica-Filled Butadiene Rubber Composites, *Plast., Rubber Compos.*, 2018, **47**(8), 345–351.

45 S. J. Stott, R. J. Mortimer, S. E. Dann, M. Oyama and F. Marken, Electrochemical Properties of Core-Shell TiC-TiO$_2$ nanoparticle Films Immobilized at ITO Electrode Surfaces, *Phys. Chem. Chem. Phys.*, 2006, **8**(46), 5437–5443.

46 M. R. Dutzer, M. C. Mangarella, J. A. Schott, S. Dai and K. S. Walton, The Effects of Reactor Design on the Synthesis of Titanium Carbide-Derived Carbon, *Chem. Eng. Sci.*, 2017, **160**, 191–199.

47 X. H. Wang and Y. C. Zhou, Oxidation Behavior of TiC-Containing Ti$_3$AlC$_2$ Based Material at 500-900 °C in Air, *Mater. Res. Innovations*, 2003, **7**(6), 381–390.